Organometallic Complexes for Nonlinear Optics. 8.[1] Syntheses and Molecular Quadratic Hyperpolarizabilities of Systematically Varied (Triphenylphosphine)gold *σ*-Arylacetylides: X-ray Crystal Structures of Au(C≡CR)(PPh_3) (R = 4-$C_6H_4NO_2$, 4,4′-$C_6H_4C_6H_4NO_2$)

Ian R. Whittall and Mark G. Humphrey*

Department of Chemistry, Australian National University, Canberra, ACT 0200, Australia

Stephan Houbrechts and André Persoons

Centre for Research on Molecular Electronics and Photonics, Laboratory of Chemical and Biological Dynamics, University of Leuven, Celestijnenlaan 200D, B-3001 Leuven, Belgium

David C. R. Hockless

Research School of Chemistry, Australian National University, Canberra, ACT 0200, Australia

Received August 8, 1996[⊗]

The series of complexes Au(C≡CR)(PPh_3) (R = Ph (**2**), 4-$C_6H_4NO_2$ (**3**), 4,4′-$C_6H_4C_6H_4NO_2$ (**4**), (*E*)-4,4′-$C_6H_4CH{=}CHC_6H_4NO_2$ (**5**), (*Z*)-4,4′-$C_6H_4CH{=}CHC_6H_4NO_2$ (**6**), 4,4′-$C_6H_4C{\equiv}CC_6H_4$-NO_2 (**7**), 4,4′-$C_6H_4N{=}CHC_6H_4NO_2$ (**8**)) have been synthesized by reaction of AuCl(PPh_3) with the corresponding acetylene and methoxide, and complexes **3**−**8** have been structurally characterized. The molecular first hyperpolarizabilities for the complexes have been determined by hyper-Rayleigh scattering at 1064 nm. Introduction of the nitro substituent (in proceeding from **2** to **3**) leads to a significant increase in nonlinearity. Experimental β values increase as **3** < **4** < **6** ≈ **7** < **8** < **5** consistent with nonlinearity increasing with (i) chain lengthening, (ii) replacing biphenyl (**4**) or yne linkage (**7**) by ene linkage (**5**), (iii) replacing (*Z*)-ene stereochemistry (**6**) with (*E*)-ene stereochemistry (**5**), and (iv) ene linkage (**5**) being more efficient than imino linkage (**8**). The same trend is observed with two-level-corrected data. A linear correlation of both experimentally-determined and two-level-corrected nonlinearities of the acetylides with precursor acetylenes is observed.

Introduction

The optical nonlinearities of organometallic complexes have been of recent interest, but the majority of investigations have dealt with bulk material responses; significantly fewer studies have considered molecular responses, an understanding of which is needed for rational materials improvement.[2−4] Among the vast panoply of organometallic complexes investigated for their nonlinear optical merit, metal acetylide complexes have attracted significant interest for both second-order[5−10] and third-order[11−14] performance, due in part to their ease of synthesis, their environmental stability, and (in the case of *trans*-bis(acetylide) complexes) their potential as "building blocks" for oligomeric and polymeric materials. We have been probing the possibility that structural modifications of metal acetylide complexes may modify optical nonlinearities in a systematic fashion and recently reported molecular quadratic optical nonlinearities (by electric field induced second harmonic generation (EFISH) and hyper-Rayleigh scattering (HRS)) of systematically-varied (cyclopentadienyl)bis(triphenylphosphine)ruthenium acetylide complexes.[5] HRS afforded results consistent with those

* To whom correspondence should be addressed. E-mail: Mark.Humphrey@anu.edu.au.

[⊗] Abstract published in *Advance ACS Abstracts,* December 1, 1996.

(1) Part 7: McDonagh, A. M.; Cifuentes, M. P.; Whittall, I. R.; Humphrey, M. G.; Samoc, M.; Luther-Davies, B.; Hockless, D. C. R. *J. Organomet. Chem*., in press.

(2) Nalwa, H. S. *Appl. Organomet. Chem*. **1991**, *5*, 349.

(3) Marder, S. R. In *Inorganic Materials*, Bruce, D. W., O'Hare, D., Eds.; Wiley: Chichester, England, 1992; p 115.

(4) Long, N. J. *Angew. Chem., Int. Ed. Engl.* **1995**, *34*, 21.

(5) Whittall, I. R.; Humphrey, M. G.; Persoons, A.; Houbrechts, S. *Organometallics* **1996**, *15*, 1935.

(6) Whittall, I. R.; Humphrey, M. G.; Hockless, D. C. R.; Skelton, B. W.; White, A. H. *Organometallics* **1995**, *14*, 3970.

(7) McDonagh, A. M.; Whittall, I. R.; Humphrey, M. G.; Skelton, B. W.; White, A. H. *J. Organomet. Chem*. **1996**, *519*, 229.

(8) McDonagh, A. M.; Whittall, I. R.; Humphrey, M. G.; Hockless, D. C. R.; Skelton, B. W.; White, A. H. *J. Organomet. Chem*. **1996**, *523*, 33.

(9) Fyfe, H. B.; Mlekuz, M.; Stringer, G.; Taylor, N. J.; Marder, T. B. In *Inorganic and Organometallic Polymers with Special Properties*; Laine, R. M., Ed.; Kluwer: Dordrecht, The Netherlands, 1992; p 331.

(10) Marder, T. B.; Lesley, G.; Yuan, Z.; Fyfe, H. B.; Chow, P.; Stringer, G.; Jobe, I. R.; Taylor, N. J.; Williams, I. D.; Kurtz, S. K. In *Materials for Nonlinear Optics: Chemical Perspectives*; Marder, S. R., Sohn, J. E., Stucky, G. D., Eds.; American Chemical Society: Washington, DC, 1991; p 605.

(11) Whittall, I. R.; Humphrey, M. G.; Samoc, M.; Swiatkiewicz, J.; Luther-Davies, B. *Organometallics* **1995**, *14*, 5493.

(12) Page, H.; Blau, W.; Davey, A. P.; Lou, X.; Cardin, D. J. *Synth. Met.* **1994**, *63*, 179.

(13) Davey, A. P.; Cardin, D. J.; Byrne, H. J.; Blau, W. In *Organic Molecules for Nonlinear Optics and Photonics*; Messier, J., Kajzar, F., Prasad, P., Eds.; Kluwer: Dordrecht, The Netherlands, 1991; p 391.

(14) Davey, A. P.; Page, H.; Blau, W.; Byrne, H. J.; Cardin, D. J. *Synth. Met.* **1993**, *55*, 3980.

S0276-7333(96)00673-5 CCC: $12.00

from EFISH, suggesting a dominant β_{zzz} contributor to the observed nonlinearities, and chain lengthening from 1- to 2-ring organometallic acetylide chromophores led to an increase in nonlinearity; however, observed nonlinearities were substantially resonance-enhanced due to strong optical absorptions near the frequency doubled wavelength of 532 nm, rendering extraction of relationships between intrinsic nonlinearity and structural factors very problematic. We have now extended our studies to embrace analogous (triphenylphosphine)gold σ-acetylide complexes and report herein the syntheses, structural characterizations, and quadratic optical nonlinearities of systematically varied (4-nitroaryl)acetylides. In contrast to our earlier work, the gold complexes considered herein contain MLCT bands with absorption maxima at substantially higher energy than their ruthenium analogues; unlike the ruthenium complexes, the gold complexes are essentially optically transparent at the harmonic frequency. Problems associated with resonance enhancement are hence significantly reduced, permitting a more realistic evaluation of intrinsic off-resonance hyperpolarizabilities and assessment of the significance of varying chromophore composition on quadratic nonlinear optical merit, the first such report for the metal acetylide system.

Experimental Section

All organometallic reactions were carried out under an atmosphere of nitrogen with the use of standard Schlenk techniques; no attempt was made to exclude air during workup of organometallic products. Dichloromethane and methanol were deoxygenated. Phenylacetylene (Aldrich) was used as received. $AuCl(PPh_3)$,[15] $Au(C{\equiv}CPh)(PPh_3)$,[16,17] 4-$HC{\equiv}CC_6H_4NO_2$,[18] 4,4′-$HC{\equiv}CC_6H_4C_6H_4NO_2$,[19] (*E*)- and (*Z*)-4,4′-$HC{\equiv}CC_6H_4CH{=}CHC_6H_4NO_2$,[20] 4,4′-$HC{\equiv}CC_6H_4C{\equiv}CC_6H_4NO_2$,[19] and 4,4′-$HC{\equiv}CC_6H_4N{=}CHC_6H_4NO_2$[5] were prepared by following the literature methods. Mass spectra were recorded using a VG ZAB 2SEQ instrument (30 kV Cs^+ ions, current 1 mA, accelerating potential 8 kV, 3-nitrobenzyl alcohol matrix) at the Research School of Chemistry, Australian National University; peaks are reported as *m*/*z* (assignment, relative intensity). Microanalyses were carried out at the Research School of Chemistry, Australian National University. Infrared spectra were recorded using a Perkin-Elmer System 2000 FT-IR spectrometer. UV-visible spectra were recorded using a Cary 5 spectrophotometer. ^1H, ^{13}C, and ^{31}P NMR spectra were recorded using a Varian Gemini-300 FT NMR spectrometer and are referenced to residual $CHCl_3$ (7.24 ppm), $CDCl_3$ (77.0 ppm), or external 85% H_3PO_4 (0.0 ppm), respectively. Spectral assignments follow the numbering scheme shown in Figure 1.

Characterization of Au(C≡CPh)(PPh$_3$) (2). Complex **2** was prepared by the literature method.[16,17] UV−vis: λ (cyclohexane) 300, 291, 276 nm; (thf) 296 nm, ϵ 13 000 M^{-1} cm^{-1}, 282 nm, ϵ 30 000 M^{-1} cm^{-1}, 268 nm, ϵ 27 000 M^{-1} cm^{-1}; (CH_3CN) 282, 268 nm. ^{13}C NMR (δ, 75 MHz, $CDCl_3$): 104.2 (br, C_2), 124.8 (C_3), 126.8 (C_6), 127.9 (C_5), 129.1 (d, J_{CP} = 11 Hz, C_m), 129.6 (d, J_{CP} = 56 Hz, C_i), 131.5 (C_p), 131.5 (C_4), 134.2 (d, J_{CP} = 14 Hz, C_o). ^{31}P NMR (δ, 121 MHz, $CDCl_3$): 43.1. FAB MS [*m*/*z* (fragment, relative intensity)]: 1019 ([M + Au$(PPh_3)]^+$, 50), 721 ($[Au(PPh_3)_2]^+$, 42), 561 ($[M + H]^+$, 23), 459 ($[M - C{\equiv}CPh]^+$, 100).

Au(4-C≡CC$_6$H$_4$NO$_2$)(PPh$_3$) (3). $AuCl(PPh_3)$ (50 mg, 0.10 mmol) and 4-$HC{\equiv}CC_6H_4NO_2$ (18 mg, 0.12 mmol) were stirred in a solution of sodium methoxide in methanol (10 mL, 0.10 M) for 16 h, after which time a pale yellow solid precipitated and was collected by filtration (51 mg, 83%). Anal. Calc for $C_{26}H_{19}AuNO_2P$: C, 51.59; H, 3.16; N, 2.31. Found: C, 51.83; H, 2.92; N, 2.47. IR (CH_2Cl_2): ν(C≡C) 2116 cm^{-1}. UV−vis: λ (cyclohexane) 336 nm; (thf) 338 nm, ϵ 25 000 M^{-1} cm^{-1}; (CH_3CN) 332 nm. ^1H NMR (δ, 300 MHz, $CDCl_3$): 7.40−7.60 (m, 17H, Ph, H_4), 8.10 (d, J_{HH} = 9 Hz, 2H, H_5). ^{13}C NMR (δ, 75 MHz, $CDCl_3$): 123.4 (C_5), 129.2 (d, J_{CP} = 11 Hz, C_m), 129.4 (d, J_{CP} = 56 Hz, C_i), 131.7 (C_p), 132.2 (C_3), 132.8 (C_4), 134.3 (d, J_{CP} = 14 Hz, C_o), 145.9 (C_6). ^{31}P NMR (δ, 121 MHz, $CDCl_3$): 42.7. FAB MS [*m*/*z* (fragment, relative intensity)]: 1064 ([M + Au$(PPh_3)]^+$, 18), 721 ($[Au(PPh_3)_2]^+$, 41), 606 ($[M + H]^+$, 11), 459 ($[M - C{\equiv}CC_6H_4NO_2]^+$, 100). Crystals of **3** suitable for diffraction analysis were grown by slow diffusion of hexane into a benzene solution at room temperature.

Au(4,4′-C≡CC$_6$H$_4$C$_6$H$_4$NO$_2$)(PPh$_3$) (4). $AuCl(PPh_3)$ (100 mg, 0.20 mmol) and 4,4′-$HC{\equiv}CC_6H_4C_6H_4NO_2$ (57 mg, 0.24 mmol) were dissolved in dichloromethane (5 mL). A methanol solution of sodium methoxide (6 mL, 0.50 mol L^{-1}) was added, and the mixture was stirred at room temperature for 16 h. Removal of the dichloromethane under reduced pressure precipitated a yellow microcrystalline product, which was filtered off and recrystallized from dichloromethane/ethanol to afford yellow crystals (116 mg, 84%). Anal. Calc for $C_{32}H_{23}AuNO_2P$: C, 56.40; H, 3.40; N, 2.06. Found: C, 56.19; H, 3.10; N, 1.76. IR (CH_2Cl_2): ν(C≡C) 2115 cm^{-1}. UV−vis: λ (cyclohexane) 350, 291, 276 nm; (thf) 350 nm, ϵ 29 000 M^{-1} cm^{-1}, 287 nm, ϵ 18 000 M^{-1} cm^{-1}, 274 nm, ϵ 19 000 M^{-1} cm^{-1}; (CH_3CN) 341, 283, 268 nm. ^1H NMR (δ, 300 MHz, $CDCl_3$):

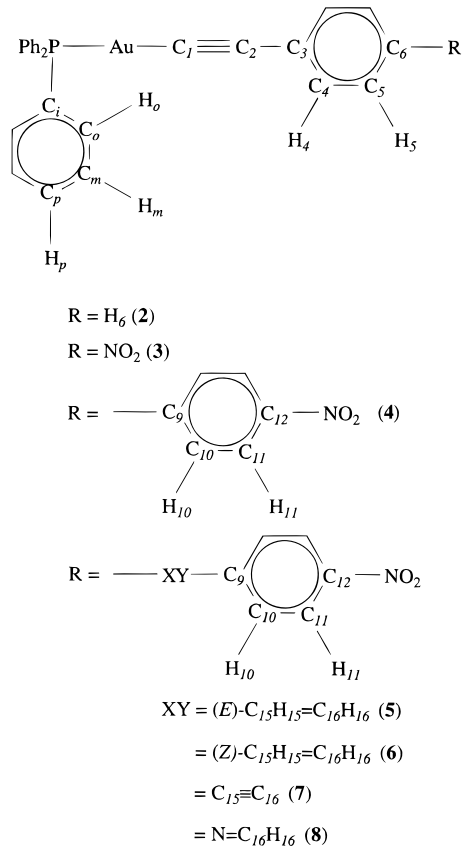

Figure 1. Numbering scheme for NMR spectral assignments.

(15) Bruce, M. I.; Nicholson, B. K.; Bin Shawkataly, O. *Inorg. Synth.* **1989**, *26*, 324.
(16) Cross, R.; Davidson, M. F.; McLennan, A. J. *J. Organomet. Chem.* **1984**, *265*, C37.
(17) Bruce, M. I.; Horn, E.; Matisons, J. G.; Snow, M. R. *Aust. J. Chem.* **1984**, *37*, 1163.
(18) Takahashi, S.; Kuroyama, Y.; Sonogashira, K.; Hagihara, N. *Synthesis* **1980**, 627.
(19) Whittall, I. R.; Cifuentes, M. P.; Humphrey, M. G.; Luther-Davies, B.; Samoc, M.; Houbrechts, S.; Persoons, A.; Heath, G. A.; Hockless, D. C. R. Manuscript in preparation.
(20) Hockless, D. C. R.; Whittall, I. R.; Humphrey, M. G. *Acta Crystallogr. C* **1996**, in press.

7.40−7.63 (m, 19H, Ph, H_4, H_5), 7.71 (d, J_{HH} = 9 Hz, 2H, H_{10}), 8.26 (d, J_{HH} = 9 Hz, 2H, H_{11}). ^{13}C NMR (δ, 75 MHz, $CDCl_3$): 124.1 (C_{11}), 125.8 (C_3), 127.0, 127.5 (C_5, C_{10}), 129.2 (d, J_{CP} = 11 Hz, C_m), 129.6 (d, J_{CP} = 56 Hz, C_i, partly obscured by C_m), 131.6 (C_p), 133.0 (C_4), 134.3 (d, J_{CP} = 14 Hz, C_o), 136.7 (C_6), 146.9 (C_9), 147.1 (C_{12}). ^{31}P NMR (δ, 121 MHz, $CDCl_3$): 43.0. FAB MS [*m*/*z* (fragment, relative intensity)]: 1140 ([M + Au(PPh$_3$)]$^+$, 9), 782 ([M + H]$^+$, 18), 721 ([Au(PPh$_3$)$_2$]$^+$, 18), 459 ([M − C≡CC$_6$H$_4$C$_6$H$_4$NO$_2$]$^+$, 100). Crystals of **4** suitable for diffraction analysis were grown by slow diffusion of ethanol into a dichloromethane solution at room temperature.

Au((*E*)-4,4′-C≡CC$_6$H$_4$CH═CHC$_6$H$_4$NO$_2$)(PPh$_3$) (5). (*E*)-4,4′-HC≡CC$_6$H$_4$CH═CHC$_6$H$_4$NO$_2$ (30 mg, 0.12 mmol) was dissolved in a 1:1 mixture of acetone and dichloromethane (5 mL). AuCl(PPh$_3$) (59 mg, 0.12 mmol) and a methanol solution of sodium methoxide (5 mL, 0.5 mol L^{-1}) were added, and the mixture was stirred at room temperature for 16 h. Removal of the dichloromethane and acetone under reduced pressure precipitated a yellow microcrystalline product, which was collected by filtration (73 mg, 85%). Anal. Calc for $C_{34}H_{25}AuNO_2P$: C, 57.71; H, 3.57; N, 1.98. Found: C, 57.16; H, 3.34; N, 2.11. IR (CH_2Cl_2): ν(C≡C) 2112 cm^{-1}. UV−vis: λ (thf) 386 nm, ϵ 38 000 M^{-1} cm^{-1}, 303 nm, ϵ 20 000 M^{-1} cm^{-1}; (CH_3CN) 376, 301 nm. ^{1}H NMR (δ, 300 MHz, $CDCl_3$): 7.08 (d, J_{HH} = 16 Hz, 1H, H_{15}), 7.21 (d, J_{HH} = 16 Hz, 1H, H_{16}), 7.41−7.61 (m, 21H, Ph, H_4, H_5, H_{10}), 8.19 (d, J_{HH} = 9 Hz, 2H, H_{11}). ^{13}C NMR (δ, 75 MHz, $CDCl_3$): 124.1 (C_{11}), 125.4 (C_3), 126.0 (C_{15}), 126.7, 126.8 (C_5, C_{10}), 129.1 (d, J_{CP} = 11 Hz, C_m), 129.5 (d, J_{CP} = 56 Hz, C_i), 131.6 (C_p), 132.8 (C_4), 133.0 (C_{16}), 134.3 (d, J_{CP} = 14 Hz, C_o), 134.5 (C_6), 143.9 (C_9), 146.6 (C_{12}). ^{31}P NMR (δ, 121 MHz, $CDCl_3$): 43.0. FAB MS [*m*/*z* (fragment, relative intensity)]: 721 ([Au(PPh$_3$)$_2$]$^+$, 70), 708 ([M + H]$^+$, 29), 459 ([M − C≡CC$_6$H$_4$CH═CHC$_6$H$_4$NO$_2$]$^+$, 100).

Au((*Z*)-4,4′-C≡CC$_6$H$_4$CH═CHC$_6$H$_4$NO$_2$)(PPh$_3$) (6). AuCl(PPh$_3$) (100 mg, 0.20 mmol) and (*Z*)-4,4′-HC≡CC$_6$H$_4$CH═CHC$_6$H$_4$NO$_2$ (60 mg, 0.24 mmol) were dissolved in dichloromethane (5 mL). A methanol solution of sodium methoxide (6 mL, 0.50 mol L^{-1}) was added, and the mixture was stirred at room temperature for 16 h. The solvent volume was reduced to 2 mL to afford a yellow microcrystalline solid, which was collected and recrystallized from dichloromethane/ethanol (113 mg, 80%). Anal. Calc for $C_{34}H_{25}AuNO_2P$: C, 57.71; H, 3.57; N, 1.98. Found: C, 57.40; H, 3.36; N, 1.79. IR (CH_2Cl_2): ν(C≡C) 2114 cm^{-1}. UV−vis: λ (cyclohexane) 369, 301 nm; (thf) 362 nm, ϵ 20 000 M^{-1} cm^{-1}, 298 nm, ϵ 28 000 M^{-1} cm^{-1}; (CH_3CN) 360, 292 nm. ^{1}H NMR (δ, 300 MHz, $CDCl_3$): 6.54 (d, J_{HH} = 12 Hz, 1H, H_{15}), 6.74 (d, J_{HH} = 12 Hz, 1H, H_{16}), 7.08 (d, J_{HH} = 9 Hz, 2H, H_4), 7.36 (d, J_{HH} = 9 Hz, 2H, H_{10}), 7.37 (d, J_{HH} = 9 Hz, 2H, H_5), 7.41−7.56 (m, 15H, Ph), 8.04 (d, J_{HH} = 9 Hz, 2H, H_{11}). ^{13}C NMR (δ, 75 MHz, $CDCl_3$): 123.5 (C_{11}), 124.5 (C_3), 127.8 (C_{15}), 128.5, 129.6 (C_5, C_{10}), 129.1 (d, J_{CP} = 11 Hz, C_m), 129.6 (d, J_{CP} = 56 Hz, C_i), 131.6 (C_p), 132.4 (C_4), 133.6 (C_{16}), 134.2 (d, J_{CP} = 14 Hz, C_o), 134.4 (C_6), 144.1 (C_9), 146.4 (C_{12}). ^{31}P NMR (δ, 121 MHz, $CDCl_3$): 43.0. FAB MS [*m*/*z* (fragment, relative intensity)]: 1166 ([M + Au(PPh$_3$)]$^+$, 11), 721 ([Au(PPh$_3$)$_2$]$^+$, 19), 708 ([M + H]$^+$, 31), 459 ([M − C≡CC$_6$H$_4$CH═CHC$_6$H$_4$NO$_2$]$^+$, 100).

Au(4,4′-C≡CC$_6$H$_4$C≡CC$_6$H$_4$NO$_2$)(PPh$_3$) (7). AuCl(PPh$_3$) (50 mg, 0.10 mmol) and 4,4′-HC≡CC$_6$H$_4$C≡CC$_6$H$_4$NO$_2$ (30 mg, 0.12 mmol) were dissolved in dichloromethane (10 mL). A methanol solution of sodium methoxide (3 mL, 0.50 mol L^{-1}) was added, and the mixture was stirred at room temperature for 16 h. Removal of the dichloromethane under reduced pressure precipitated a yellow microcrystalline powder (58 mg, 82%). Anal. Calc for $C_{34}H_{23}AuNO_2P$: C, 57.88; H. 3.29; N, 1.99. Found: C, 57.60; H, 3.15; N, 1.95. IR (CH_2Cl_2): ν(C≡C) 2115 cm^{-1}. UV−vis: λ (cyclohexane) 361, 303 nm; (thf) 362 nm, ϵ 36 000 M^{-1} cm^{-1}, 301 nm, ϵ 32 000 M^{-1} cm^{-1}; (CH_3CN) 355, 298 nm. ^{1}H NMR (δ, 300 MHz, $CDCl_3$): 7.41−7.57 (m, 19H, Ph, H_4, H_5), 7.62 (d, J_{HH} = 9 Hz, 2H, H_{10}), 8.19 (d, J_{HH} = 9 Hz, 2H, H_{11}). ^{13}C NMR (δ, 75 MHz, $CDCl_3$): 120.1 (C_6), 123.5 (C_{11}), 126.0 (C_3), 129.2 (d, J_{CP} = 11 Hz, C_m), 129.5 (d, J_{CP} = 56 Hz, C_i), 131.6 (C_p), 131.9 (C_9), 131.5, 132.2, 132.4 (C_4, C_5, C_{10}), 134.3 (d, J_{CP} = 14 Hz, C_o), 146.8 (C_{12}). ^{31}P NMR (δ, 121 MHz, $CDCl_3$): 43.0. FAB MS [*m*/*z* (fragment, relative intensity)]: 1164 ([M + Au(PPh$_3$)]$^+$, 8), 721 ([Au(PPh$_3$)$_2$]$^+$, 27), 706 ([M + H]$^+$, 16), 459 ([M − C≡CC$_6$H$_4$C≡CC$_6$H$_4$NO$_2$]$^+$, 100).

Au(4,4′-C≡CC$_6$H$_4$N═CHC$_6$H$_4$NO$_2$)(PPh$_3$) (8). AuCl(PPh$_3$) (50 mg, 0.10 mmol) and 4,4′-HC≡CC$_6$H$_4$N═CHC$_6$H$_4$NO$_2$ (30 mg, 0.12 mmol) were dissolved in dichloromethane (5 mL). A methanol solution of sodium methoxide (5 mL, 0.50 M) was added, and the mixture was stirred at room temperature for 16 h. Removal of the dichloromethane under reduced pressure precipitated a yellow microcrystalline powder, which was recrystallized from dichloromethane/ethanol to afford yellow crystals (60 mg, 85%). Anal. Calc for $C_{33}H_{24}AuN_2O_2P$: C, 55.94; H, 3.42; N, 3.95. Found: C, 56.06; H, 3.24; N, 3.82. IR (CH_2Cl_2): ν(C≡C) 2115 cm^{-1}. UV−vis: λ (thf) 392 nm, ϵ 21 000 M^{-1} cm^{-1}, 297 nm, ϵ 32 000 M^{-1} cm^{-1}; (CH_3CN) 377, 290 nm. ^{1}H NMR (δ, 300 MHz, $CDCl_3$): 7.17 (d, J_{HH} = 8 Hz, 2H, H_4), 7.40−7.60 (m, 17H, Ph, H_5), 8.04 (d, J_{HH} = 9 Hz, 2H, H_{10}), 8.30 (d, J_{HH} = 9 Hz, 2H, H_{11}), 8.54 (s, 1H, H_{16}). ^{13}C NMR (δ, 75 MHz, $CDCl_3$): 120.9 (C_5), 123.9 (C_3), 124.0 (C_{11}), 129.1 (d, J_{CP} = 11 Hz, C_m), 129.3 (C_{10}), 129.6 (d, J_{CP} = 56 Hz, C_i), 131.6 (C_p), 133.3 (C_4), 134.3 (d, J_{CP} = 14 Hz, C_o), 141.6 (C_9), 149.0, 149.1 (C_6, C_{12}). ^{31}P NMR (δ, 121 MHz, $CDCl_3$): 43.0. FAB MS [*m*/*z* (fragment, relative intensity)]: 1167 ([M + Au(PPh$_3$)]$^+$, 13), 721 ([Au(PPh$_3$)$_2$]$^+$, 31), 709 ([M + H]$^+$, 22), 459 ([M − C≡CC$_6$H$_4$N═CHC$_6$H$_4$NO$_2$]$^+$, 100).

Table 1. Crystallographic Data for Complexes 3 and 4

	3	**4**
empirical formula	$C_{26}H_{19}AuNO_2P$	$C_{32}H_{23}AuNO_2P$
M_r	605.38	681.48
cryst color, habit	yellow, block	pale yellow, prism
cryst dimens (mm^3)	0.2 × 0.2 × 0.1	0.4 × 0.2 × 0.1
space group	$P2_1/c$ (No. 14)	$P\bar{1}$ (No. 2)
a (Å)	8.650(3)	8.818(3)
b (Å)	18.555(5)	9.810(3)
c (Å)	14.179(2)	15.649(4)
α (deg)		84.18(2)
β (deg)	91.15(2)	89.55(2)
γ (deg)		89.43(3)
V (Å^3)	2275.3(8)	1346.7(6)
Z	4	2
D_{calc} (g cm^{-3})	1.767	1.681
μ (cm^{-1})	65.81 (Mo Kα)	55.31 (Mo Kα)
transm factors	0.71−1.00	0.67−1.00
secondary extinction	9(5) × 10^{-9}	none
N	4179	4781
N_o ($I > 3.00\sigma(I)$)	2800	3774
no. variables	281	334
p-factor	0.001	0.001
R	0.024	0.029
R_w	0.017	0.032

X-ray Structure Determinations. Unique diffractometer data sets were obtained using the $\omega-2\theta$ scan technique (graphite-monochromated Mo Kα radiation; 0.710 69 Å; $2\theta_{max}$ = 50.1°; 295 K) and yielded *N* independent reflections, N_o of these with $I \geq 3.00\sigma(I)$ being considered "observed" and used in full matrix least-squares refinement; an empirical ψ-type absorption correction was applied in each case. Anisotropic thermal parameters were refined for the non-hydrogen atoms; (x, y, z, U_{iso})$_H$ were included constrained at estimated values. Conventional residuals *R* and R_w on |*F*| are given; the weighting function $w = 4F_o^2/\sigma^2(F_o^2)$, where $\sigma^2(F_o^2) = [S^2(C + 4B) + (pF_o^2)^2]/Lp^2$ (S = scan rate, C = peak count, B = background count, p = p factor determined experimentally from standard reflections), was employed. Computation used the teXsan package.[21] Specific data collection, solution, and refinement parameters are given in Table 1. Pertinent

(21) *Single Crystal Structure Analysis Software, Version 1.6c*; Molecular Structure Corp.: The Woodlands, TX, 1993.

results are given in the figures and tables. Tables of atomic coordinates and thermal parameters and complete lists of bond lengths and angles for non-hydrogen atoms have been deposited at the Cambridge Crystallographic Data Centre.

HRS Measurements. An injection-seeded Nd:YAG laser (Q-switched Nd:YAG Quanta Ray GCR5, 1064 nm, 8 ns pulses, 10 pps) was focused into a cylindrical cell (7 mL) containing the sample. The intensity of the incident beam was varied by rotation of a half-wave plate placed between crossed polarizers. Part of the laser pulse was sampled by a photodiode to measure the vertically polarized incident light intensity. The frequency doubled light was collected by an efficient condenser system under 90° and detected by a photomultiplier. The harmonic scattering and linear scattering were distinguished by appropriate filters; gated integrators were used to obtain intensities of the incident and harmonic scattered light. All measurements were performed in thf using *p*-nitroaniline ($\beta = 21.4 \times 10^{-30}$ cm^5 esu^{-1})[22] as a reference. Further details of the experimental procedure have been reported elsewhere.[23,24]

Results and Discussion

Synthesis and Characterization of Gold Acetylide Complexes. The new acetylide complexes were prepared by extension of literature procedures[16,17] or modifications thereof (Scheme 1) and were characterized by IR, ^{1}H, ^{13}C, and ^{31}P NMR spectroscopies, mass spectrometry, and satisfactory microanalyses. For **3**−**8**, characteristic ν(C≡C) in the solution IR spectra (CH_2Cl_2 solvent) between 2112 and 2116 cm^{-1} and phosphine P in the ^{31}P NMR between 42.7 and 43.1 ppm are relatively insensitive to variations in the acetylide ligand. The previously unreported ^{13}C NMR spectrum for **2** contains a broad resonance at 104.2 ppm assigned to the β-carbon but no resonance assignable to a metal-bound carbon. Neither Au−C nor AuC≡*C* was detected in the ^{13}C NMR spectra for the new complexes. The lack of an observable α-carbon resonance in **2** or acetylide carbon resonances in the spectra of **3**−**8** may be due to quadrupolar broadening by the 100% abundant ^{197}Au nucleus. The mass spectra for **3**−**8** all show peaks corresponding to protonation of the molecular ion and fragmentation by loss of acetylide, together with peaks assigned to phosphine auration of the molecular ion and $[Au(PPh_3)_2]^+$; in all cases, [M − acetylide]$^+$ is the most intense signal.

The UV−visible spectra for complexes **3**−**8** are characterized by intense (ϵ = 13 000−38 000 M^{-1} cm^{-1}) MLCT bands at lowest frequency together with higher energy bands assigned to σ(Au←P) → π^*(PPh) (see below). Replacement of aryl 4-H by 4-NO_2 in the phenylacetylide ligand in proceeding from **2** to **3** results in a red shift of 42 nm in λ_{max}; a similar replacement for Ru(4-C≡CC_6H_4R)$(PPh_3)_2(\eta$-$C_5H_5)$ (R = H, NO_2) resulted in a 130 nm shift to lower energy. Chain lengthening of the acetylide chromophore leads as expected to a bathochromic shift of the MLCT band with **5** and **8** containing the lowest energy transitions. All new complexes display negative solvatochromism, in contrast to our previously reported (cyclopentadienyl)-bis(phosphine)ruthenium acetylides where positive solvatochromism was observed.[6] The magnitudes of the solvatochromic shifts are small in magnitude (≤10 nm in proceeding from cyclohexane to acetonitrile solvent) compared to the large shifts (up to 50 nm across the same range of solvents) obtained with the related ruthenium acetylides.

Scheme 1

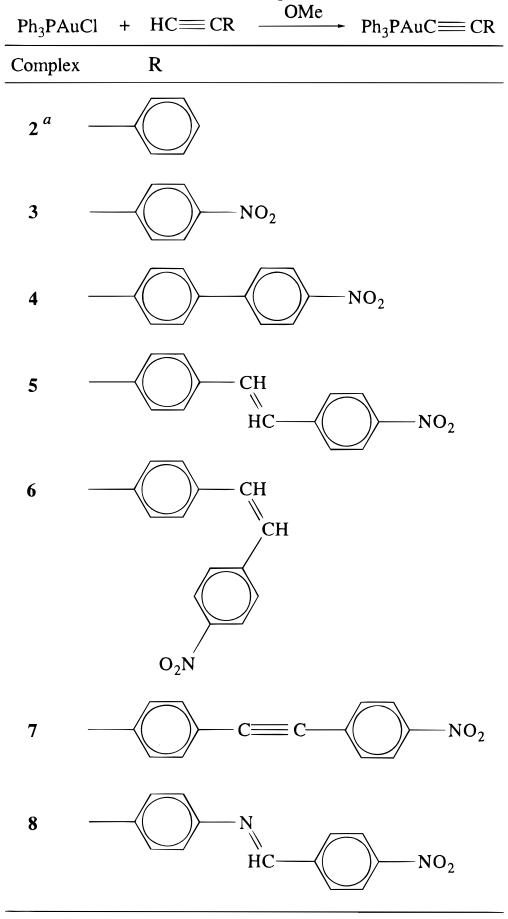

Footnote: [a] References 16 and 17.

X-ray Structural Studies. We have completed X-ray diffraction studies on complexes **3**−**8**; complete details of those for **5**−**8** will be reported elsewhere.[25] Crystallographic data are collected in Table 1; important bond lengths are shown in Table 2, and selected angles, in Table 3. ORTEP plots are displayed in Figures 2 (**3**) and 3 (**4**).

The structural determinations confirm the molecular composition inferred from spectral data. The Au−P(1)

(22) Stähelin, M.; Burland, D. M.; Rice, J. E. *Chem. Phys. Lett.* **1992**, *191*, 245.
(23) Clays, K.; Persoons, A. *Rev. Sci. Instrum.* **1992**, *63*, 3285.
(24) Hendrickx, E.; Dehu, C.; Clays, K.; Brédas, J. L.; Persoons, A. In *Polymers for Second-Order Nonlinear Optics*; Lindsay, G. A., Singer, K. D., Eds.; ACS Symposium Series 601; American Chemical Society: Washington, DC, 1995; p 82.
(25) Whittall, I. R.; Humphrey, M. G.; Hockless, D. C. R. Manuscript in preparation.
(26) Li, D.; Hong, X.; Che, C.; Lo, W.; Peng, S. *J. Chem. Soc., Dalton Trans.* **1993**, 2929.
(27) Kaharu, T.; Ishii, R.; Adachi, T.; Yoshida, T.; Takahashi, S. *J. Mater. Chem.* **1995**, *5*, 687.
(28) Corfield, P. W. R.; Shearer, H. M. M. *Acta Crystallogr.* **1967**, *23*, 156.
(29) Jia, G.; Payne, N. C.; Vittal, J. J.; Puddephatt, R. J. *Organometallics* **1993**, *12*, 4771.
(30) Jia, G.; Puddephatt, R. J.; Vittal, J. J.; Payne, N. C. *Organometallics* **1993**, *12*, 263.
(31) Bruce, M. I.; Duffy, D. N. *Aust. J. Chem.* **1986**, *39*, 1697.
(32) Müller, T. E.; Wing-Kin Choi, S.; Mingos, D. M. P.; Murphy, D.; Williams, D. J.; Wing-Wah Yam, V. *J. Organomet. Chem.* **1994**, *484*, 209.
(33) Shieh, S.; Hong, X.; Peng, S.; Che, C. *J. Chem. Soc., Dalton Trans.* **1994**, 3067.

Table 2. Important Bond Lengths (Å) for (Triphenylphosphine)gold Acetylide Complexes 3 and 4

bond	3	4	bond	3	4
Au(1)−P(1)	2.277(1)	2.273(2)	C(3)−C(8)	1.400(7)	1.351(9)
Au(1)−C(1)	1.973(5)	1.992(6)	C(4)−C(5)	1.380(7)	1.408(9)
P(1)−C(111)	1.808(6)	1.807(6)	C(5)−C(6)	1.365(8)	1.360(9)
P(1)−C(121)	1.798(5)	1.823(6)	C(6)−C(7)	1.377(8)	1.356(8)
P(1)−C(131)	1.828(5)	1.816(6)	C(6)−C(9)		1.487(8)
O(1)−N(1)	1.213(7)	1.192(8)	C(7)−C(8)	1.374(7)	1.379(9)
O(2)−N(1)	1.228(7)	1.207(8)	C(9)−C(10)		1.345(8)
N(1)−C(6)	1.492(7)		C(9)−C(14)		1.371(9)
N(1)−C(12)		1.480(8)	C(10)−C(11)		1.386(8)
C(1)−C(2)	1.206(6)	1.192(7)	C(11)−C(12)		1.362(9)
C(2)−C(3)	1.446(6)	1.441(8)	C(12)−C(13)		1.35(1)
C(3)−C(4)	1.390(7)	1.343(9)	C(13)−C(14)		1.390(9)

distances [2.277(1) Å (**3**), 2.273(2) Å (**4**)] are similar, and all P−C distances close to 1.8 Å as expected; other intra-arylphosphine bond lengths and angles are also unexceptional. Our primary interest in these structural studies is in variations in Au−acetylide bond length and angle parameters as the nature of the acetylide ligand is changed. P(1)−Au(1)−C(1) angles [178.1(2)° (**3**), 174.2(2)° (**4**)] are close to linearity, Au−C(1) vectors [1.973(5) Å (**3**), 1.992(7) Å (**4**)] are similar, C(1)−C(2) distances [1.200(6) Å (**3**), 1.192(7) Å (**4**)] are experimentally equivalent within the error margins, and Au−C(1)−C(2) angles [175.1(5)° (**3**), 173.5(6) (**4**)] deviate only slightly from linearity. Differences in other intra-acetylide ligand parameters between the complexes are marginal; the ground-state geometry in the solid state is very similar for **3** and **4**, with both complexes possessing a "bond-alternated" AuC≡CC(aryl) rather than Au=C=C=C(aryl) geometry.

Table 4 collects cognate data from structurally characterized gold acetylide analogues including results from the structural studies on **5**−**8**, ordered by Au−C(1) distance. With the exception of the imprecisely determined $(Au(C{\equiv}CPh))_2(\mu\text{-dppe})$, little variation in the Au−C(1) parameter is observed for phosphine-ligated gold acetylides. In particular, the introduction of an electron-withdrawing nitro substituent to the arylacetylide ligand has little effect on this bond distance (perfluorination of the phenylacetylide group similarly has no effect on this parameter). Almost half of the related previously reported gold(I) acetylide crystal structures contain short Au···Au contacts, believed to result from a weak relativistic bonding force.[34] The most interesting comparison for the present complexes is with $Au(C{\equiv}CPh)(PPh_3)$[31] and $Au(C{\equiv}CC_6F_5)(PPh_3)$.[17] The crystal structure of the former contains nearly orthogonal molecules with short Au···Au separations, a situation which does not exist in the latter or with complex **3**. The reason for this with $Au(C{\equiv}CC_6F_5)(PPh_3)$ and other nonconforming previously reported gold(I) acetylides may be steric but is almost certainly electronic with complex **3**, there being no appreciable increase in steric requirements on introduction of the 4-nitro substituent.

Quadratic Hyperpolarizabilities. We have determined the molecular quadratic hyperpolarizabilities of complexes **1**−**8** together with those of the (nitroaryl)-acetylene precursors; the results of the HRS measurements[38] are given in Table 5, together with previously reported data for related (cyclopentadienyl)bis(phosphine)ruthenium complexes.[5] Due to the small difference between the second-harmonic signals of the solvent and a concentrated solution of **1**, the molecular quadratic optical nonlinearity β_{1064} for the chloro complex **1** ($\leq 3.5 \times 10^{-30}$ cm^5 esu^{-1}) can only be seen as an estimated upper limit. Complex **2**, obtained by replacement of the chloro ligand by a phenylacetylide group, has β_{1064} large for a compound which can be considered as a phenyl group containing a donor substituent ($Ph_3PAuC{\equiv}C$) only (for a range of donor-substituted benzenes, Cheng *et al.* found negligible nonlinearities β_{1900} for all substituents other than NMe_2 (1.1×10^{-30} cm^5 esu^{-1}, neat) and julolidine (1.3×10^{-30} cm^5 esu^{-1}, dioxane solvent) and concluded that all donors evaluated were ineffective in inducing charge and polarizability asymmetry).[39] (*E*)-4-$H_2NC_6H_4CH{=}CHPh$ is reported to have a β value of 7.4×10^{-30} cm^5 esu^{-1},[39] and acetylene linkages have been shown to be less effective than ethylene ones for asymmetric polarizability in organic compounds;[40] it is therefore certain that $Ph_3PAuC{\equiv}C$ is a donor of comparable efficiency (at least) to 4-$H_2NC_6H_4C{\equiv}C$. Replacement of the 4-arylacetylide H in **2** by a nitro substituent to generate the donor−acceptor acetylide complex **3** leads to a substantial increase in nonlinearity, with efficiency similar to that of 4-nitroaniline (21.4×10^{-30} cm^5 esu^{-1}, thf solvent)[22] and 4,4′-$H_2NC_6H_4C{\equiv}CC_6H_4NO_2$ (24×10^{-30} cm^5 esu^{-1}, $CHCl_3$ solvent).[40]

The current work permits examination of the effect of chain lengthening on optical nonlinearity of donor−acceptor metal acetylide complexes, with **3** < **4** < **6** ≈ **7** < **8** < **5**. These data are consistent with an increase in nonlinearity for "extended chain" 2-ring organometallic acetylide chromophores versus 1-ring complexes, confirming our observation in the ruthenium system.[5] A recent examination of bimetallic sesquifulvalene complexes suggested that β_{1064}(yne linkage) >> β_{1064}(ene linkage) and β_o(yne linkage) ≈ β_o(ene linkage) (2-level corrected) for varying sesquifulvalene bridging functionalities;[41] data were substantially resonance enhanced, raising doubts about the comparable efficiencies of ene and yne linkages. Examination of the effect of varying carbon-containing bridges in the "extended" 2-ring complexes in the present work reveals an efficiency sequence $C_6H_4C_6H_4 \approx C_6H_4C{\equiv}CC_6H_4 < C_6H_4CH{=}CHC_6H_4$ for C-containing bridges; unlike the bimetallic sesquifulvalene system, the linear optical absorption bands for the gold acetylides are significantly removed from the harmonic frequency, suggesting that this relative ordering accurately reflects off-resonance nonlinearities. Torsion effects at the phenyl−phenyl linkage (for biphenyl compounds) and orbital energy mismatch of p orbitals of sp-hybridized acetylenic carbons with p orbitals of sp^2-hybridized phenyl carbons

(34) Payne, N. C.; Ramachandran, R.; Puddephatt, R. L. *Can. J. Chem.* **1995**, *73*, 6.
(35) Jia, G.; Puddephatt, R. J.; Scott, J. D.; Vittal, J. J. *Organometallics* **1993**, *12*, 3565.
(36) Bruce, M. I.; Grundy, K. R.; Liddell, M. J.; Snow, M. R.; Tiekink, E. R. T. *J. Organomet. Chem.* **1988**, *344*, C49.
(37) Carriedo, G. A.; Riera, V.; Solans, X.; Solans, J. *Acta Crystallogr. C* **1988**, *C44*, 978.
(38) The experimental methodology employed for HRS has been reported previously: see ref 23 and references cited therein.
(39) Cheng, L.-T.; Tam, W.; Stevenson, S. H.; Meredith, G. R.; Rikken, G.; Marder, S. R. *J. Phys. Chem.* **1991**, *95*, 10631.
(40) Cheng, L.-T.; Tam, W.; Marder, S. R.; Stiegman, A. E.; Rikken, G.; Spangler, C. W. *J. Phys. Chem.* **1991**, *95*, 10643.
(41) Behrens, U.; Brussaard, H.; Hagenau, U.; Heck, J.; Hendrickx, E.; Körnich, J.; van der Linden, J. G. M.; Persoons, A.; Spek, A. L.; Veldman, N.; Voss, B.; Wong, H. *Chem. Eur. J.* **1996**, *2*, 98.

Table 3. Important Angles (deg) for (Triphenylphosphine)gold Acetylide Complexes 3 and 4

angle	3	4	angle	3	4
P(1)−Au(1)−C(1)	178.1(2)	174.2(2)	C(3)−C(4)−C(5)	120.9(6)	121.2(7)
Au(1)−P(1)−C(111)	113.3(2)	112.9(2)	C(4)−C(5)−C(6)	118.2(6)	121.9(7)
Au(1)−P(1)−C(121)	114.1(2)	116.3(2)	C(5)−C(6)−C(7)	122.9(5)	115.7(6)
Au(1)−P(1)−C(131)	112.3(2)	111.8(2)	C(5)−C(6)−C(9)		121.7(6)
C(111)−P(1)−C(121)	104.6(3)	104.1(3)	C(7)−C(6)−C(9)		122.5(6)
C(111)−P(1)−C(131)	105.7(3)	105.0(3)	C(6)−C(7)−C(8)	118.8(6)	122.0(7)
C(121)−P(1)−C(131)	106.0(2)	105.6(3)	C(3)−C(8)−C(7)	120.1(5)	122.5(6)
O(1)−N(1)−O(2)	125.7(6)	124.2(7)	C(6)−C(9)−C(10)		123.5(6)
O(1)−N(1)−C(12)		118.3(8)	C(6)−C(9)−C(14)		119.9(6)
O(2)−N(1)−C(12)		117.5(8)	C(10)−C(9)−C(14)		116.5(6)
O(1)−N(1)−C(6)	117.4(7)		C(9)−C(10)−C(11)		123.0(7)
O(2)−N(1)−C(6)	116.8(7)		C(10)−C(11)−C(12)		117.9(7)
Au(1)−C(1)−C(2)	175.1(5)	173.5(6)	N(1)−C(12)−C(11)		119.5(7)
C(1)−C(2)−C(3)	179.8(6)	177.0(7)	N(1)−C(12)−C(13)		118.3(8)
C(2)−C(3)−C(4)	121.0(6)	122.2(6)	C(11)−C(12)−C(13)		122.2(7)
C(2)−C(3)−C(8)	119.9(6)	121.1(6)	C(12)−C(13)−C(14)		117.4(8)
C(4)−C(3)−C(8)	119.0(4)	116.6(6)	C(9)−C(14)−C(13)		123.0(7)

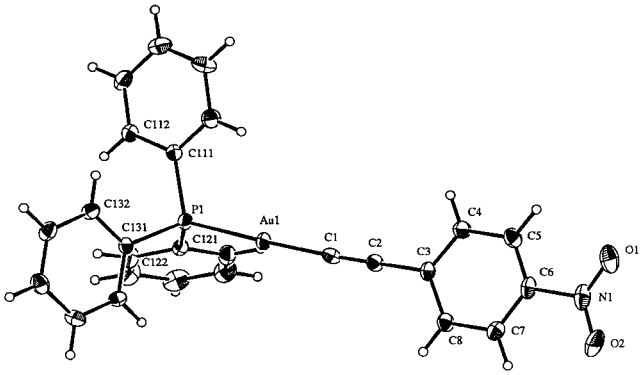

Figure 2. Molecular structure and atomic labeling scheme for Au(4-C≡$CC_6H_4NO_2$)(PPh_3) (**3**), with 20% thermal ellipsoids shown for the non-hydrogen atoms. Hydrogen atoms have arbitrary radii.

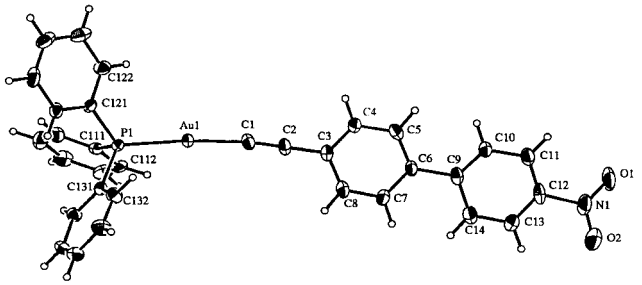

Figure 3. Molecular structure and atomic labeling scheme for Au(4,4′-C≡$CC_6H_4C_6H_4NO_2$)(PPh_3) (**4**), with 20% thermal ellipsoids shown for the non-hydrogen atoms. Hydrogen atoms have arbitrary radii.

(for diphenylacetylene compounds) have been suggested as reasons for lower β for $C_6H_4C_6H_4$- and $C_6H_4C{\equiv}CC_6H_4$-linked organic compounds, compared with their *trans*-stilbene analogues;[40] it is likely that the same factors influence relative nonlinearities for "extended-chain" acetylide complexes, as the trend in the nonlinear optical merit for the gold acetylides mirrors that of the organic compounds.

Observed nonlinearities suggest that $\beta[(Z)] < \beta[(E)]$ for bridge stereochemistry variation in the C_6H_4-CH=CHC_6H_4-linked complexes; although it is tempting to ascribe this variation to dipole moment differences (the molecular geometry of the *E* isomer leads to an increased charge separation compared to the *Z* isomer), the relevant optical transition in the *E* isomer is almost twice as intense as that for the *Z* isomer, and a combination of these effects is likely. The difference in intrinsic nonlinearity between the *Z* and *E* isomers is likely to be substantially greater than that observed experimentally; the *Z* form fluoresces significantly at the frequency doubled wavelength, inflating its observed nonlinearity compared to that of the *E* isomer.[42] The present work also permits comment on the effects of bridge atom variation on observed nonlinearity; the experimentally determined nonlinearity for the (*E*)-imino complex **8** is about two-thirds that of the (*E*)-ene-linked complex **5**. ZINDO-derived nonlinearities for related Ru((*E*)-4,4′-C≡CC_6H_4X=$CHC_6H_4NO_2$)$(PPh_3)_2$(η-C_5H_5) were similar (55×10^{-30} cm^5 esu^{-1}, X = N; 45×10^{-30} cm^5 esu^{-1}, X = CH), while the experimentally-determined values (840×10^{-30} cm^5 esu^{-1}, X = N; 1455×10^{-30} cm^5 esu^{-1}, X = CH) were substantially resonance enhanced and hence difficult to utilize for structure−property studies;[5] the present work demonstrates that ene linkage is more effective than imino linkage at maximizing nonlinearity in these organometallic acetylide chromophores and is consistent with related EFISH-derived results for an organic system (a doubling of nonlinearity for (*E*)-4,4′-$MeOC_6H_4X$=$CHC_6H_4NO_2$ in proceeding from X = N (14×10^{-30} cm^5 esu^{-1}) to X = CH (28×10^{-30} cm^5 esu^{-1})).[39]

Table 5 also includes the two-level-corrected values, with β_o about half β_{1064} for the gold acetylide complexes. It should be emphasized that the two-state model may not be adequate for these donor−acceptor organometallic systems. The two-state model has been found to be useful when dealing with a restricted class of compounds where structural modifications are directed at the charge-transfer band which may contribute to the hyperpolarizability.[39] Although this criterion applies to the gold complexes considered herein, it may not be useful where two dominant optical transitions are close to 2ω, as is the case for **4**−**8** (by analogy with previous work on ethynylgold(I) complexes,[32,43] the higher energy bands (λ < 310 nm) are probably due to σ(Au←P) → π^*-(PPh) transitions; the low nonlinearities for **1** and **2** suggest that these transitions do not significantly influence the observed nonlinearities for **3**−**8**, and any contribution that they make is likely to be consistent across the series of complexes). For the present series

(42) Problems with fluorescence interfering with hyper-Rayleigh scattering measurements have been noted recently: Morrison, I. D.; Denning, R. G.; Laidlaw, W. M.; Stammers, M. A. *Rev. Sci. Instrum.* **1996**, *67*, 1445, and ref 24.

(43) Yam, V. W.-W.; Choi, S. W.-K.; Cheung, K.-K. *Organometallics* **1996**, *15*, 1734.

Table 4. Selected Geometric Parameters in Existing Analogues

complex	Au−C(1) (Å)	C(1)−C(2) (Å)	C(2)−C(3) (Å)	shortest Au···Au separation (Å)	Au−C(1)−C(2) (deg)	C(1)−C(2)−C(3) (deg)	ref
$(Au(C{\equiv}CPh))_2(\mu\text{-dppe})$	1.87(3)	1.16(4)	1.46(4)	3.153(2)	168(3)	177(3)	26
	2.00(3)	1.21(4)	1.42(4)	3.153(2)	177(2)	180(2)	
$Au(4\text{-}C{\equiv}CC_6H_4O(CO)\text{-}4'\text{-}C_6H_4OCH(Me)\text{-}C_6H_{13}{}^n)(C{\equiv}NCH_2CH(Et)Bu^n)$	1.92[a]	1.23[a]	1.45[a]	4.418(2)	179[a]	179[a]	27
$Au(C{\equiv}CPh)(NH_2Pr^i)$	1.935(19)	1.210(28)	1.479(28)	3.274[a]	174(2)	179(2)	28
$Au(C{\equiv}CBu^t)(C{\equiv}N\text{-}3\text{-}Me\text{-}4\text{-}C_6H_3C{\equiv}CH)$	1.955(10)	1.206(15)	1.463(16)	3.479(2)	173.6(10)	173.9(12)	29, 30
$Au(4,4'\text{-}C{\equiv}CC_6H_4C{\equiv}CC_6H_4NO_2)(PPh_3)$ (**7**)	1.96(2)	1.22(2)	1.48(2)	>5	169(1)	177(2)	25
	2.00(1)	1.21(2)	1.44(2)	>5	172(1)	178(2)	
$Au(C{\equiv}CPh)(PPh_3)$ (**2**)	1.97(2)	1.18(2)	1.46(2)	3.379(1)	175.7(16)	176.5(18)	31
	2.02(2)	1.16(2)	1.47(2)	3.379(1)	170.8(19)	174.0(20)	
$Au(4\text{-}C{\equiv}CC_6H_4NO_2)(PPh_3)$ (**3**)	1.973(5)	1.206(6)	1.446(6)	>5	175.1(5)	179.8(6)	this work
$C_2(Au(P(naphthyl)Ph_2)_2{\cdot}2CHCl_3$	1.983(8)	1.222(16)	*b*	*c*	174.2(10)	*b*	32
$C_2(Au(P(naphthyl)_2Ph)_2{\cdot}6CHCl_3$	1.986(17)	1.225(34)	*b*	*c*	177.8(23)	*b*	32
$(Au(C{\equiv}CPh))_2(\mu\text{-}2,5\text{-bis-(diphenylphosphino)pyridine})$	1.988(12)	1.199(17)	*d*	3.252(1)	172.5(11)	*d*	33
$Au(4,4'\text{-}C{\equiv}CC_6H_4N{=}CHC_6H_4NO_2)(PPh_3)$ (**8**)	1.989(9)	1.18(1)	1.44(1)	>5	168(1)	175(1)	25
	1.99(1)	1.19(1)	1.46(1)	>5	172(1)	176(1)	
$Au((Z)\text{-}4,4'\text{-}C{\equiv}CC_6H_4CH{=}CHC_6H_4NO_2)\text{-}(PPh_3)$ (**6**)	1.99(1)	1.23(1)	1.44(1)	>5	176(1)	176(1)	25
$(Au(C{\equiv}CBu^t))_2(\mu\text{-dppm})$	1.990(10)	1.192(12)	1.483(14)	3.3307(9)	173.5(9)	176.5(11)	34
	2.005(9)	1.197(11)	1.464(13)	3.3307(9)	173.1(8)	177.5(10)	
$Au(4,4'\text{-}C{\equiv}CC_6H_4C_6H_4NO_2)(PPh_3)$ (**4**)	1.992(6)	1.192(7)	1.441(8)	>5	173.5(6)	177.0(7)	this work
$Au(C{\equiv}CC_6F_5)(PPh_3)$	1.993(14)	1.197(16)	1.442(20)	>5	175.4(10)	178.4(12)	17
$(Au(C{\equiv}CPh))_2(\mu\text{-}4,4'\text{-}C_6H_4C_6H_4(PPr^i{}_2)_2)$	1.997(9)	1.179(11)	1.451(11)	*c*	172.7(9)	177.2(9)	35
$C_2(Au(PPh_3))_2{\cdot}C_6H_6$	2.00(1)	1.19(2)	*b*	*c*	180	*b*	36
$C_2(Au(P(ferrocenyl)_2Ph)_2{\cdot}4EtOH$	2.002(6)	1.196(12)	*b*	*c*	177.9(11)	*b*	32
$C_2(Au(P(3\text{-}tolyl)_3))_2{\cdot}C_6H_6$	2.002(9)	1.19(2)	*b*	*c*	180	*b*	36
$Au((E)\text{-}4,4'\text{-}C{\equiv}CC_6H_4CH{=}CHC_6H_4NO_2)$ (PPh_3) (**5**)	2.009(6)	1.200(7)	1.443(7)	>5	168.4(5)	174.3(6)	25
	2.013(5)	1.192(7)	1.445(7)	>5	168.4(5)	175.2(6)	
$Au(C{\equiv}CPh)(P(ferrocenyl)_2Ph)$	2.011(15)	1.172(21)	1.478(22)	*c*	176.9(13)	179.4(15)	32
$C_2(Au(P(3\text{-}tolyl)_3))_2$	2.02(1)	1.13(2)	*b*	*c*	180	*b*	36
$Au(C{\equiv}CPh)(P(4\text{-}tolyl)_3)$	2.024(2)	1.169(3)	1.474(4)	*d*	170.3(2)	178.2(3)	37

[a] Estimated standard deviation not quoted. [b] Not applicable. [c] No close Au−Au contact. [d] Not quoted.

Table 5. Experimental Nonlinear Optical Response and Linear Optical Spectroscopic Parameters[a]

compd	λ (nm) (ϵ (10^4 L mol^{-1} cm^{-1}))	β (10^{-30} cm^5 esu^{-1}) exptl[b]	β (10^{-30} cm^5 esu^{-1}) corrctd[c]
$Au(C{\equiv}CPh)(PPh_3)$ (**2**)	296 (1.3), 282 (3.0), 268 (2.7)	6	4
$Au(4\text{-}C{\equiv}CC_6H_4NO_2)(PPh_3)$ (**3**)	338 (2.5)	22	12
$Au(4,4'\text{-}C{\equiv}CC_6H_4C_6H_4NO_2)(PPh_3)$ (**4**)	350 (2.9), 287 (1.8), 274 (1.9)	39	20
$Au((E)\text{-}4,4'\text{-}C{\equiv}CC_6H_4CH{=}CHC_6H_4NO_2)(PPh_3)$ (**5**)	386 (3.8), 303 (2.0)	120	49
$Au((Z)\text{-}4,4'\text{-}C{\equiv}CC_6H_4CH{=}CHC_6H_4NO_2)(PPh_3)$ (**6**)	362 (2.0), 298 (2.8)	58	28
$Au(4,4'\text{-}C{\equiv}CC_6H_4C{\equiv}CC_6H_4NO_2)(PPh_3)$ (**7**)	362 (3.6), 301 (3.2)	59	28
$Au(4,4'\text{-}C{\equiv}CC_6H_4N{=}CHC_6H_4NO_2)(PPh_3)$ (**8**)	392 (2.1), 297 (3.2)	85	34
$Ru(4\text{-}C{\equiv}CC_6H_4NO_2)(PPh_3)_2(\eta\text{-}C_5H_5)$[c]	460 (1.1), 382 (1.1)	468	96
$Ru(4\text{-}C{\equiv}CC_6H_4NO_2)(PMe_3)_2(\eta\text{-}C_5H_5)$[c]	477 (1.7), 279 (1.0)	248	39
$Ru((E)\text{-}4,4'\text{-}C{\equiv}CC_6H_4CH{=}CHC_6H_4NO_2)(PPh_3)_2(\eta\text{-}C_5H_5)$[c]	476 (2.6), 341 (2.4)	1455	232
$Ru(4,4'\text{-}C{\equiv}CC_6H_4N{=}CHC_6H_4NO_2)(PPh_3)_2(\eta\text{-}C_5H_5)$[c]	496 (1.3), 298 (2.6)	840	86
$4\text{-}HC{\equiv}CC_6H_4NO_2$	288 (1.5)	14	9
$4,4'\text{-}HC{\equiv}CC_6H_4C_6H_4NO_2$	316 (2.1)	21	12
$(E)\text{-}4,4'\text{-}HC{\equiv}CC_6H_4CH{=}CHC_6H_4NO_2$	358 (3.3), 282 (1.3)	55	27
$(Z)\text{-}4,4'\text{-}HC{\equiv}CC_6H_4CH{=}CHC_6H_4NO_2$	336 (1.2), 268 (2.0)	16	9
$4,4'\text{-}HC{\equiv}CC_6H_4C{\equiv}CC_6H_4NO_2$	331 (2.8), 273 (1.8)	31	17
$4,4'\text{-}HC{\equiv}CC_6H_4N{=}CHC_6H_4NO_2$	355 (1.4), 270 (1.9)	36	18

[a] Solutions in thf. [b] HRS at 1.06 μm; all values ±10%. [c] HRS experimental data corrected for resonance enhancement using the two-level model with $\beta_o = \beta[1 - (2\lambda_{max}/1064)^2][1 - (\lambda_{max}/1064)^2]$; damping factors not included. [d] Reference 5.

of complexes, the relative ordering for observed and two-level-corrected β are the same, and all complexes are optically transparent at 2ω; it is therefore almost certain that the effects of structural modification on observed nonlinearity reflect their effect upon intrinsic nonlinearity.

Figure 4 correlates uncorrected and two-level-corrected optical nonlinearities of the gold acetylide complexes with wavelength of the important MLCT band. Not surprisingly, there is a dramatic increase in uncorrected nonlinearity with increase in λ_{max} across this series of complexes, and a smaller, but still significant, increase in the two-level-corrected values with increase in λ_{max}. The Ph_3PAu and H moieties are related in an isolobal fashion,[44] and a comparison of the effect of this isolobal replacement was of interest; Table 5 also contains optical nonlinearities for the precursor acetylenes, which in all cases are substantially lower than those of the acetylide derivatives. Figure 5 charts the relationship between optical nonlinearities of acetylene and acetylide complex. With the exception of the (*Z*)-ene-linked compounds (for which the acetylide was

(44) Hoffmann, R. *Angew. Chem., Int. Ed. Engl.* **1982**, *21*, 711.

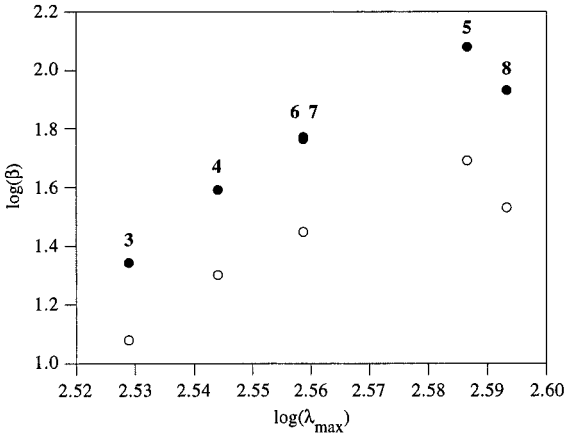

Figure 4. Dependence of the molecular quadratic hyperpolarizability for complexes **3**−**8** upon the wavelength of the dominant optical transition: ●, uncorrected; ○, two-level corrected. Units: β in 10^{-30} cm^5 esu^{-1}, λ_{max} in nm.

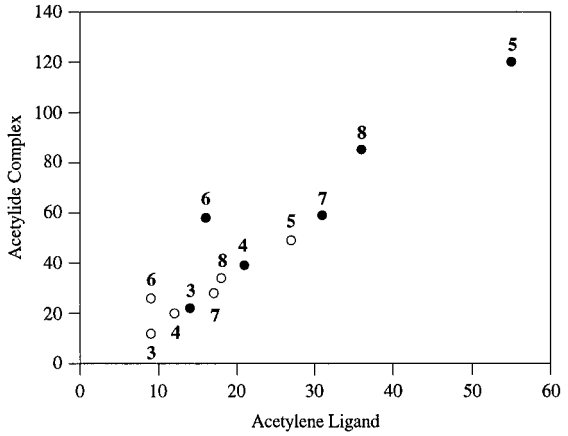

Figure 5. Correlation of molecular quadratic hyperpolarizabilities of complexes **3**−**8** with those of the corresponding acetylenes: ● uncorrected; ○ two-level corrected. Units: 10^{-30} cm^5 esu^{-1}.

observed to fluoresce significantly; see above), a linear correlation for both uncorrected and two-level-corrected data is observed. The slopes of these graphs (2.4 (R = 0.99) for uncorrected; 2.0 (R = 0.99) for two-level-corrected) define a "figure of merit" for the ligated gold center compared to the hydrogen.

No attempt has been made to optimize the efficiency of the organometallic donor in the current series of complexes; the focus has been on relating structural components to variation in nonlinear optical merit. Although our previous data for ruthenium acetylide complexes were substantially resonance enhanced, their absolute values (both experimentally-observed and two-level-corrected) are much larger than those for the gold complexes considered herein. This is consistent with the 18 valence electron, more oxidizable, ruthenium(II) being a better donor than the 14 valence electron, less oxidizable, gold(I). Nevertheless, the Ph_3PAu unit has comparable efficiency to the strongest organic donors (4-aminophenyl; see above), suggesting that oxidizable 18 valence electron organometallic complexes can provide access to stronger donors than are possible in organic systems, potentially leading to enhanced nonlinearities. Further studies with systematically varied complexes are currently underway.

Acknowledgment. We thank the Australian Research Council (M.G.H.), Telstra (M.G.H.), the Belgian Government (Grant No. IUAP-16) (A.P.), the Belgian National Science Foundation (Grant Nos. G.2103.93, 9.0012.92, and 9.0011.92) (A.P.), and the University of Leuven (Grant No. GOA 95/1) (A.P.) for support of this work. I.R.W. is the recipient of an Australian Postgraduate Research Award (Industry), M.G.H. holds an ARC Australian Research Fellowship, and S.H. is a Research Assistant of the Belgian National Fund for Scientific Research. Mr. D. Bogsanyi is thanked for obtaining the UV−visible spectra.

Supporting Information Available: Tables giving final values of all refined atomic coordinates, all calculated atomic coordinates, all anisotropic and isotropic thermal parameters, and all bond lengths and angles for complexes **3** and **4** (30 pages). Ordering information is given on any current masthead page.

OM960673J